

# SEISMIC CHARACTERIZATION OF VERTICAL FRACTURES DESCRIBED AS GENERAL LINEAR-SLIP INTERFACES

VLADIMIR GRECHKA<sup>1</sup>, ANDREY BAKULIN<sup>2</sup> and ILYA TSVANKIN<sup>1</sup>

<sup>1</sup>Center for Wave Phenomena, Department of Geophysics,  
Colorado School of Mines, Golden, CO 80401-1887, USA

<sup>2</sup>Schlumberger Cambridge Research, High Cross, Madingley Road,  
Cambridge, CB3 0EL, England

## Summary

Fluid flow in many hydrocarbon reservoirs is controlled by aligned fractures which make the medium anisotropic on the scale of seismic wavelength. Applying the linear slip theory of Schoenberg and co-workers, we investigate the effective triclinic medium produced by a single set of the most general vertical fractures. The “generality” of our model means the allowance for coupling between the normal (to the fracture plane) stress and the tangential jump in displacement (and vice versa). Despite the low symmetry of the model, it possesses several distinct features which help to estimate both the fracture and background parameters using seismic data. For example, the polarization vector of the vertically propagating fast shear wave  $S_1$  and the semi-major axis of the  $S_1$ -wave normal-moveout (NMO) ellipse from horizontal reflectors always point in the direction of the fracture strike. Moreover, for the  $S_1$ -wave both the vertical velocity and the NMO velocity along the fractures are equal to the shear-wave velocity in the host rock.

Analysis of the effective anisotropic parameters allows us to identify the seismic signatures needed for unambiguous fracture characterization. The input seismic data sufficient for estimating the fracture parameters may include the NMO ellipses from horizontal reflectors and the vertical velocities of  $P$ - and two split  $S$ -waves, combined with the  $P$ -wave slowness surface reconstructed from multiazimuth walkaway VSP data.

## Introduction

The problem of fracture characterization using seismic data can be divided into two main parts. First, it is necessary to obtain the so-called *effective* model formed by fractures with given microstructural parameters embedded in a specified host (unfractured) rock. A convenient framework for modeling the effective elastic parameters of fractured formations is provided by the linear slip theory of Schoenberg (1980). Second, one has to identify the seismic signatures which are sufficiently sensitive to the fracture parameters to ensure a stable inversion procedure. Bakulin et al. (2000a,b,c) devised seismic fracture-characterization algorithms for several typical fractured models, from transversely isotropic with a horizontal symmetry axis (HTI) to monoclinic.

Here those results are extended to the effective medium produced by the most general (in terms of the linear slip theory) parallel vertical fractures in a purely isotropic host rock. The coupling between the normal stress and the tangential jump in displacement (and vice versa), accounted for by our model, may be caused by either micro-corrugation of fracture faces (e.g., Bakulin et al., 2000c) or misalignment between the fracture strike and the principal axes of stress (Nakagawa et al., 2000). Although such a model has the lowest possible symmetry, it is described by only *eight* independent parameters (in the properly rotated coordinate frame), which facilitates the development of fracture-characterization methods based on seismic data.

## Effective model of a general fracture set

According to the linear slip theory (Schoenberg, 1980), the effective compliance matrix  $\mathbf{s}$  of a fractured medium can be expressed as the sum of the background compliance  $\mathbf{s}_b$  and the excess fracture compliance  $\mathbf{s}_f$ . For a single set of vertical fractures with the normals parallel to the  $x_1$ -axis, the compliance  $\mathbf{s}_f$  is given by

$$\mathbf{s}_f = \begin{pmatrix} K_N & 0 & 0 & 0 & K_{NV} & K_{NH} \\ 0 & 0 & 0 & 0 & 0 & 0 \\ 0 & 0 & 0 & 0 & 0 & 0 \\ 0 & 0 & 0 & 0 & 0 & 0 \\ K_{NV} & 0 & 0 & 0 & K_V & K_{VH} \\ K_{NH} & 0 & 0 & 0 & K_{VH} & K_H \end{pmatrix}. \quad (1)$$

The compliances  $K_N$ ,  $K_V$ ,  $K_H$ ,  $K_{NV}$ ,  $K_{NH}$  and  $K_{VH}$  appear in the boundary conditions of the so-called linear slip which relate the jumps in displacement across the fracture plane to the corresponding traction (stress) components. It is convenient to describe fractures by the dimensionless weaknesses defined as

$$\begin{aligned}\Delta_N &= \frac{(\lambda + 2\mu) K_N}{1 + (\lambda + 2\mu) K_N}, & \Delta_V &= \frac{\mu K_V}{1 + \mu K_V}, & \Delta_H &= \frac{\mu K_H}{1 + \mu K_H}, \\ \Delta_{NV} &= \frac{\sqrt{\mu(\lambda + 2\mu)} K_{NV}}{1 + \sqrt{\mu(\lambda + 2\mu)} K_{NV}}, & \Delta_{NH} &= \frac{\sqrt{\mu(\lambda + 2\mu)} K_{NH}}{1 + \sqrt{\mu(\lambda + 2\mu)} K_{NH}}, \\ \Delta_{VH} &= \frac{\sqrt{\mu(\lambda + 2\mu)} K_{VH}}{1 + \sqrt{\mu(\lambda + 2\mu)} K_{VH}}.\end{aligned}\quad (2)$$

Assuming that the fracture density and, consequently, the weaknesses are small, the effective stiffness matrix  $\mathbf{c}$  can be simplified by linearizing its components in the weaknesses:

$$\mathbf{c} \equiv (\mathbf{s}_b + \mathbf{s}_f)^{-1} = \begin{pmatrix} c_{11} & \kappa c_{11} & \kappa c_{11} & 0 & c_{15} & c_{16} \\ \kappa c_{11} & c_{22} & c_{23} & 0 & \kappa c_{15} & \kappa c_{16} \\ \kappa c_{11} & c_{23} & c_{22} & 0 & \kappa c_{15} & \kappa c_{16} \\ 0 & 0 & 0 & c_{44} & 0 & 0 \\ c_{15} & \kappa c_{15} & \kappa c_{15} & 0 & c_{55} & c_{56} \\ c_{16} & \kappa c_{16} & \kappa c_{16} & 0 & c_{56} & c_{66} \end{pmatrix}, \quad (3)$$

where

$$\begin{aligned}c_{11} &\approx (\lambda + 2\mu)(1 - \Delta_N), & c_{15} &\approx -\Delta_{NV} \sqrt{\mu(\lambda + 2\mu)}, & c_{16} &\approx -\Delta_{NH} \sqrt{\mu(\lambda + 2\mu)}, \\ c_{22} &\approx (\lambda + 2\mu)(1 - \kappa^2 \Delta_N), & c_{23} &\approx \lambda(1 - \kappa \Delta_N), & c_{44} &= \mu, \\ c_{55} &\approx \mu(1 - \Delta_V), & c_{56} &\approx -\mu \Delta_{VH} \sqrt{\frac{\mu}{\lambda + 2\mu}}, & c_{66} &\approx \mu(1 - \Delta_H), & \kappa &= \frac{\lambda}{\lambda + 2\mu}.\end{aligned}\quad (4)$$

Here  $\lambda$  and  $\mu$  are the Lamé constants of the host rock (background), which determine the background velocities of  $P$ - and  $S$ -waves:

$$V_{Pb} = \sqrt{(\lambda + 2\mu)/\rho}, \quad V_{Sb} = \sqrt{\mu/\rho}; \quad (5)$$

$\rho$  is the density. Equations (4) indicate that the elements of the stiffness matrix (3) satisfy two constraints,

$$c_{22} = \kappa^2 c_{11} + 2(1 + \kappa) c_{44} = c_{23} + 2 c_{44}, \quad (6)$$

so the effective triclinic medium in the coordinate frame associated with the fractures is defined by only *eight* independent parameters.

### Seismic signatures for small fracture weaknesses

#### *Phase velocities of $P$ - and $S$ -waves in the fracture plane*

Next, we study the properties of the special type of triclinic media described by the linearized stiffness matrix (3). Solving the Christoffel equation for the phase velocities of the  $P$ - and  $S$ -waves propagating in the fracture plane  $[x_2, x_3]$  yields

$$V_P \approx V_{Pb} \left(1 - \kappa^2 \frac{\Delta_N}{2}\right), \quad V_{S1} = V_{Sb}, \quad (7)$$

$$V_{S2} \approx V_{Sb} \left[1 - \frac{1}{2} \left(\Delta_H \sin^2 \theta + \frac{V_{Sb}}{V_{Pb}} \Delta_{VH} \sin 2\theta + \Delta_V \cos^2 \theta\right)\right], \quad (8)$$

where  $\theta$  is the phase angle with the  $x_3$ -axis. Approximations (7) and (8) indicate that in the  $[x_2, x_3]$ -plane the velocities of  $P$ - and fast  $S$ -waves are almost independent of angle, while the velocity function of the slow wave  $S_2$  is approximately elliptical. Since the vertically traveling  $S_1$ - and  $S_2$ -waves are polarized within the fracture plane and orthogonal to it (respectively), their polarization directions can be used to determine the fracture orientation.

Equations (7) and (8) allow us to obtain the shear-wave splitting coefficient at vertical incidence:

$$\gamma^{(S)} \approx \frac{\Delta_V}{2}. \quad (9)$$

For penny-shaped cracks,  $\gamma^{(S)}$  is approximately equal to the crack density – a well-known result for less general fracture sets with  $\Delta_{NV} = \Delta_{NH} = \Delta_{VH} = 0$  (e.g., Bakulin et al., 2000a,b).

#### *NMO velocities from a horizontal reflector*

Consider pure-mode reflections from the bottom of a horizontal homogeneous layer with the stiffnesses determined by matrix (3). Using the results of Grechka et al. (1999), we obtain the following closed-form expressions for the  $2 \times 2$  matrices  $\mathbf{W}_{ij}$  describing the NMO ellipses of the  $P$ -,  $S_1$ - and  $S_2$ -waves:

$$\mathbf{W}^P \approx \frac{1}{V_{Pb}^2} \begin{pmatrix} 1 + \Delta_N(1 - 4g_b^2) + 4\Delta_V g_b & 2\Delta_{NH}(1 - 2g_b)\sqrt{g_b} \\ 2\Delta_{NH}(1 - 2g_b)\sqrt{g_b} & 1 + \Delta_N(1 - 2g_b)^2 \end{pmatrix}, \quad (10)$$

$$\mathbf{W}^{S_1} \approx \frac{1}{V_{Sb}^2} \begin{pmatrix} 1 + \Delta_H - \frac{\Delta_{VH}^2}{\Delta_V} g_b & 0 \\ 0 & \frac{\Delta_V}{\Delta_V} g_b \\ 0 & 1 \end{pmatrix}, \quad (11)$$

$$\mathbf{W}^{S_2} \approx \frac{1}{V_{Sb}^2} \begin{pmatrix} 1 - 3\Delta_V + 4g_b\Delta_N + \frac{\Delta_{VH}^2}{\Delta_V} g_b & 2\Delta_{NH}\sqrt{g_b} \\ 2\Delta_{NH}\sqrt{g_b} & 1 + \Delta_H \end{pmatrix}, \quad (12)$$

where

$$g_b \equiv (V_{Sb}/V_{Pb})^2. \quad (13)$$

Note that the axes of the NMO ellipse  $\mathbf{W}^{S_1}$  are parallel and perpendicular to the fractures, and its semi-major axis (the NMO velocity in the  $x_2$ -direction) is equal to the shear-wave velocity  $V_{Sb}$  in the background. Although equation (11) was derived for the linearized stiffness matrix, both statements turn out to hold for any magnitude of the fracture weaknesses.

#### *P-wave slowness surface*

It is clear from equations (7), (8) and (10)–(12) that the vertical velocities and NMO ellipses are primarily controlled by the weaknesses  $\Delta_N$ ,  $\Delta_V$ ,  $\Delta_H$  and  $\Delta_{NH}$ . If borehole data are available, the two remaining weaknesses ( $\Delta_{NV}$  and  $\Delta_{VH}$ ) can be estimated from  $P$ -wave multiazimuth walkaway VSP (vertical seismic profiling) surveys which can be used to reconstruct a portion of the  $P$ -wave slowness surface  $p_3 \equiv q = q(p_1, p_2)$ . In the limit of small weaknesses,  $q$  is given by

$$q(p_1, p_2) \approx q_b + \frac{1}{q_b} \left[ \frac{(\nu - 2g_b)^2}{2V_{Pb}^2} \Delta_N + 2p_1^2 V_{Sb}^2 (p_2^2 \Delta_H + q_b^2 \Delta_V) \right] \\ + 2p_1 \sqrt{g_b} \left[ (\nu - 2g_b) \left( \Delta_{NV} + \frac{p_2}{q_b} \Delta_{NH} \right) + 2p_1 p_2 V_{Sb}^2 \Delta_{VH} \right], \quad (14)$$

where

$$q_b = \sqrt{\frac{1}{V_{Pb}^2} - p_1^2 - p_2^2} \quad \text{and} \quad \nu = 1 - 2p_1^2 V_{Sb}^2, \quad (15)$$

Equation (14) shows that the weaknesses  $\Delta_{NV}$  and  $\Delta_{VH}$  make first-order contributions to the slowness surface  $q$ .

### **Fracture characterization**

The above analysis suggests that the vertical velocities of the  $P$ -,  $S_1$ - and  $S_2$ -waves and their NMO ellipses from horizontal reflectors constrain all background and fracture parameters, except for the weaknesses  $\Delta_{NV}$  and  $\Delta_{VH}$ . Adding  $P$ -wave multiazimuth walkaway VSP data (or a portion of the slowness surface  $q$ ) should be sufficient for recovering  $\Delta_{NV}$  and  $\Delta_{VH}$ . Here we verify those conclusions by performing actual inversion for the fracture weaknesses and background velocities based on the exact equations (Figure 1). The error bars in Figure 1 are caused by Gaussian noise with the standard deviations 0.5%, 2%, and 2% added to the vertical velocities, NMO ellipses, and  $P$ -wave slowness surface, respectively. The results give a clear confirmation of our

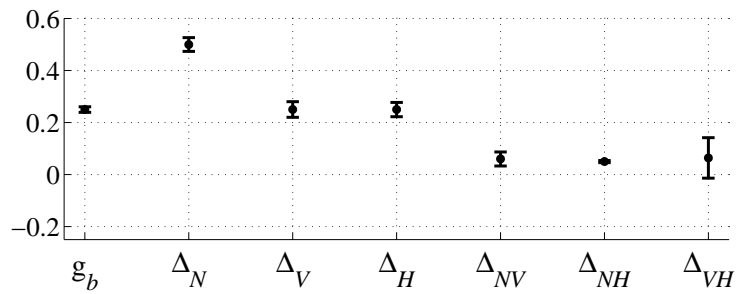


FIG. 1. Inversion of the vertical velocities and NMO ellipses of the  $P$ -,  $S_1$ - and  $S_2$ -waves and the  $P$ -wave slowness surface for the fracture and background parameters. The dots mark the correct values, the error bars correspond to the 95% confidence intervals in the estimated quantities.

analytic predictions based on the assumption of small weaknesses<sup>1</sup>. The confidence intervals for all estimated parameters except for  $\Delta_{VH}$  do not exceed 0.03 (the value obtained for  $\Delta_V$ ), which is close to relative magnitude of the noise added to the NMO velocities and  $P$ -wave slownesses.

## Discussion and conclusions

A set of parallel vertical fractures of the most general type embedded in otherwise isotropic host rock produces an effective medium of triclinic symmetry. Whereas triclinic media depend on up to 21 elastic stiffness coefficients, such a model is fully defined by the fracture azimuth and just eight independent parameters – the background coefficients  $\lambda$  and  $\mu$  and six fracture compliances. The relative simplicity of this fracture-induced triclinic anisotropy [see equation (3)] suggests that the background parameters and the fracture compliances can be found from the effective stiffnesses. The key issue in fracture characterization, however, is stable recovery of the stiffnesses themselves from seismic data.

We showed that the fracture orientation, the weaknesses  $\Delta_N$ ,  $\Delta_V$ ,  $\Delta_H$ , and  $\Delta_{NH}$ , and the background velocities  $V_{Pb}$  and  $V_{Sb}$  can be unambiguously estimated from the vertical velocities of the  $P$ -,  $S_1$ -, and  $S_2$ -waves and their NMO ellipses from horizontal reflectors. Note that the NMO ellipses of pure shear reflections can be reconstructed from  $PP$ - and  $PS$ -wave 3-D multiazimuth reflection data, so shear-wave excitation is not necessary (Grechka and Tsvankin, 2001). The two remaining weaknesses,  $\Delta_{NV}$  and  $\Delta_{VH}$ , can be obtained by inverting the  $P$ -wave slowness surface measured using  $P$ -wave multiazimuth walkaway VSP surveys. Numerical tests demonstrate that the combination of three different types of seismic data (the vertical velocities and NMO ellipses of pure-mode reflections and  $P$ -wave VSP data) tightly constrains all fracture weaknesses needed for a robust solution of the fracture-characterization problem.

## References

- Bakulin, A., Grechka, V., and Tsvankin, I., 2000a, Estimation of fracture parameters from reflection seismic data. Part I: HTI model due to a single fracture set: *Geophysics*, **65**, 1788–1802.
- Bakulin, A., Grechka, V., and Tsvankin, I., 2000b, Estimation of fracture parameters from reflection seismic data. Part II: Fractured models with orthorhombic symmetry: *Geophysics*, **65**, 1803–1817.
- Bakulin, A., Grechka, V., and Tsvankin, I., 2000c, Estimation of fracture parameters from reflection seismic data. Part III: Fractured models with monoclinic symmetry: *Geophysics*, **65**, 1818–1830.
- Grechka, V., and Tsvankin, I., 2001,  $PP + PS = SS$ : 63nd Conference of EAGE, Amsterdam, Extended Abstracts (this volume).
- Grechka, V., Tsvankin, I., and Cohen, J.K., 1999, Generalized Dix equation and analytic treatment of normal-moveout velocity for anisotropic media: *Geophysical Prospecting*, **47**, 117–148.
- Nakagawa, S., Nihei, K.T., and Myer, L.R., 2000, Shear-induced conversion of seismic wave across single fractures: *Int. J. of Rock Mech. and Mining Sci.*, **37**, N 1–2, 203–218.
- Schoenberg, M., 1980, Elastic wave behavior across linear slip interfaces: *J. Acoust. Soc. Am.*, **68**, 1516–1521.

<sup>1</sup>Note that the fracture weaknesses in this model are not small. Estimating the crack density from the shear-wave splitting coefficient [equation (9)], as is usually done for penny-shaped cracks, gives a value of 12.5%.